REPORT DOCUMENTATION PAGE

Form Approved
OMB No. 0704-0188

Public reporting burden for this collection of information is estimated to average 1 hour per response, including the time for reviewing instructions, searching existing data sources, gathering and maintaining the data needed, and completing and reviewing this collection of information. Send comments regarding this burden estimate or any other aspect of this collection of information, including suggestions for reducing this burden to Department of Defense, Washington Headquarters Services, Directorate for Information Operations and Reports (0704-0188), 1215 Jefferson Davis Highway, Suite 1204, Arlington, VA 22202-4302. Respondents should be aware that notwithstanding any other provision of law, no person shall be subject to any penalty for failing to comply with a collection of information if it does not display a currently valid OMB control number. **PLEASE DO NOT RETURN YOUR FORM TO THE ABOVE ADDRESS.**

1. REPORT DATE *(DD-MM-YYYY)* 11-06-2019	**2. REPORT TYPE** Final Report	**3. DATES COVERED** *(From - To)* 5/1/2015-6/29/2018
4. TITLE AND SUBTITLE Multi-scale Predictability with a New Coupled Non-hydrostatic global model over the Arctic.		**5a. CONTRACT NUMBER** N00014-15-1-2220
		5b. GRANT NUMBER GRANT11771147
		5c. PROGRAM ELEMENT NUMBER
6. AUTHOR(S) Steven Cavallo and William Skamarock		**5d. PROJECT NUMBER**
		5e. TASK NUMBER
		5f. WORK UNIT NUMBER
7. PERFORMING ORGANIZATION NAME(S) AND ADDRESS(ES) The Board of Regents of the University of Oklahoma 201 Stephenson Parkway Suite 3100 Five Partners Place Norman, OK 73019-9705		**8. PERFORMING ORGANIZATION REPORT NUMBER**
9. SPONSORING / MONITORING AGENCY NAME(S) AND ADDRESS(ES) Office of Naval Research 875 N. Randolph Street, Suite 1425 Arlington, VA 22203-1995		**10. SPONSOR/MONITOR'S ACRONYM(S)** ONR
		11. SPONSOR/MONITOR'S REPORT NUMBER(S)

12. DISTRIBUTION / AVAILABILITY STATEMENT

Approved for public release: distribution unlimited.

13. SUPPLEMENTARY NOTES

None

14. ABSTRACT

This study evaluates the performance of MPAS by examining a multi-scale feature that is common to the Arctic: Tropopause polar vortices (TPVs). TPVs are commonly observed tropopause-based vortices that originate in higher latitudes and are precursors to development of surface cyclones. Yet, very little is known about the role of TPVs in longer-term predictability. Higher latitude regions are a unique environment for growth and longevity of TPVs due to their relative position poleward of the polar jet stream and limited heat and moisture. Spatial scales of TPVs range as high as ~1000 km and lifetimes can exceed one month. Lifetimes can be particularly long over the Arctic Ocean during summer months when the polar jet stream has a relatively weak influence. Given their longevity in the Arctic and their active role in surface cyclone formation and growth, we hypothesize that TPVs are an important component of longer-term prediction, and hence the predictability of sea ice.

This hypothesis is tested by extending a new atmospheric nonhydrostatic dynamical core from the Model for Prediction Across Scales (MPAS) to a framework where MPAS is embedded within the Community Atmosphere Model (CAM) of the Community Earth System Model (CESM), on medium to long range weather prediction (week - months) focusing on the Arctic region. This fully-coupled atmosphere-ocean-land-sea ice modeling system, referred to as MPAS-CESM, is a global model that allows for local refinement of the horizontal grid such that there is a smooth transition in resolution from the relatively coarse global mesh to finer mesh in regions of primary interest, which in this study is the Arctic region. A hierarchy of modeling experiments are performed summers of 2006 and 2007 that evinced anticyclonic and cyclonic sea-level pressure anomalies, respectively, for a variety of mesh configurations and physical parameterizations. Results emphasize the importance of resolving TPVs over the Arctic at finer scales and their dynamical linkages to processes associated with developing

15. SUBJECT TERMS

16. SECURITY CLASSIFICATION OF:			**17. LIMITATION OF ABSTRACT**	**18. NUMBER OF PAGES**	**19a. NAME OF RESPONSIBLE PERSON**
a. REPORT	**b. ABSTRACT**	**c. THIS PAGE**			**19b. TELEPHONE NUMBER** *(include area code)*

The UNIVERSITY *of* OKLAHOMA®
Office of Research Services

May 6, 2019

Defense Technical Information Center
8725 John J Kingman Road Ste 0944
Fort Belvoir, VA 22060-6218

Dear Sir,

Enclosed is the final technical report for award #N00014-15-1-2220 for Dr. Steven Cavallo.

Thank you,

Cathi Parker
Sponsored Programs Coordinator
Office of Research Services
University of Oklahoma

201 Stephenson Parkway, Suite 3100, Norman, Oklahoma 73019
PHONE: (405) 325-4757 FAX: (405) 325-6029
EMAIL: ors@ou.edu WEBSITE: ors.ou.edu

Final Technical Report of Contract ONR N00014-15-1-2220

Multi-scale predictability with a new coupled non-hydrostatic global model over the Arctic

Prime Offeror and list of subawards:
The Board of Regents of the University of Oklahoma (OU)
University Corporation for Atmospheric Research/National Center for Atmospheric Research (UCAR/NCAR)

Principal Investigator: Dr. Steven Cavallo
University of Oklahoma School of Meteorology
120 David L. Boren Blvd. Suite 5900
Norman, OK 73072-7307
cavallo@ou.edu Ph: (405) 325-2439 Fax: (405) 325-7689

Co-Principal Investigator: Dr. William Skamarock
NCAR Earth System Laboratory, Mesoscale and Microscale Meteorology Division
P.O. Box 3000
Boulder, CO 80307-3000
skamaroc@ucar.edu Ph: (303) 497-8161 Fax: (303) 497-8171

Administrative contact:
Ms. Lawana Dillard, Sponsored Programs Coordinator
Office of Research Services
201 David L. Boren Blvd., Suite 150
Norman, OK 73019-5300
gradoral@ou.edu Ph: (405) 325-4808 Fax: (405) 325-6029

Table of Contents

LONG-TERM GOALS **3**

OBJECTIVES AND OVERVIEW 3

APPROACH 4

Model for Prediction Across Scales (MPAS) 6

A multi-scale application—Tropopause polar vortices (TPVs) 7

Short timescale variability in Arctic sea ice 9

RESULTS **10**

Atmosphere only 11

Object-based idealized experiments 14

Atmosphere, Ocean, and Sea Ice Couplings 16

IMPACT/APPLICATIONS **20**

TRANSITIONS **21**

RELATED PROJECTS **21**

REFERENCES 22

PUBLICATIONS AND PROCEEDINGS 27

PATENTS 29

HONORS/AWARDS/PRIZES 29

LONG-TERM GOALS

Atmospheric tests of a new atmospheric nonhydrostatic dynamical core from the Model for Prediction Across Scales (MPAS) are extended to a framework where MPAS is embedded within the Community Atmosphere Model (CAM) of the Community Earth System Model (CESM), on medium to long range weather prediction (week - months) focusing on the Arctic region. We subsequently refer to this fully- coupled atmosphere-ocean-land-sea ice modeling system as MPAS-CESM. MPAS is a fully compressible, nonhydrostatic, global model that allows for local refinement of the horizontal grid such that there is a smooth transition in resolution from the relatively coarse global mesh to finer mesh in regions of primary interest. Results indicate that having a smooth transition in horizontal resolution reduce complications that typically arise from traditional downscaling and nesting approaches. Additionally, since MPAS does not employ a latitude-longitude grid, it does not require the use of polar filtering and will therefore exhibit uniform performance over polar regions. Given these new capabilities available with MPAS, and the earth-system couplings of CESM, MPAS-CESM is expected to make considerable improvements in numerical predictions at weekly to monthly time scales. We have implemented meshes for the atmospheric component that are locally refined over the Arctic region which are used for multi-scale CESM simulations in this study.

MPAS and the coupled MPAS-CESM is used to examine the evolution, dynamics and predictability of summer season Arctic surface pressure anomalies that we show are associated with the dynamics of tropopause polar vortices (TPVs). The surface pressure anomalies correlate with the phase of the Arctic oscillation (AO) and the flow anomalies have a significant impact on sea ice movement and extent in the summer season. We test the ability of the atmospheric component of MPAS to simulate the evolution of TPVs in the summers of 2006 and 2007 that evinced anticyclonic and cyclonic sea-level pressure anomalies, respectively, for a variety of mesh configurations and physical parameterizations. Our results emphasize the importance of resolving TPVs over the Arctic at finer scales and their dynamical linkages to processes associated with developing surface cyclones at synoptic and sub-synoptic scales. This research examines the dynamics of these linkages and the ability of MPAS and MPAS-CESM to simulate the evolution of the coupled system. Specifically, we examine sensitivities in the evolution of the fully-coupled Arctic environment for the summers of 2006 and 2007. We address the questions: How well can MPAS predict the evolution of the 2006 TPV in free-forecasting mode? Does sea ice evolve as with the physical expectations outlined above? Do we observe the appropriate AO signature in the MPAS-CESM simulations?

OBJECTIVES AND OVERVIEW

This research, submitted under the ONR Broad Agency Announcement addresses Code 32 (Ocean Battlespace Sensing), addresses the section on Ocean, Atmosphere and Space

Research and the call for Arctic and integrated prediction. The research is in direct response to the ONR Department Research Initiative "Predictability of Seasonal and Intraseasonal Oscillations: On the pathway to a seamless earth prediction system." As directed in the initiative, we are advancing a nonhydrostatic global atmospheric model, and its variable-resolution capabilities will allow us to produce multiscale atmospheric simulations on the current generation of supercomputers. We are placing the MPAS atmospheric solver in CESM, and thus will be testing a full Earth System Model (i.e. coupled models) in our work as called for in the DRI. We are addressing scientific issues related to Arctic weather and the Arctic Oscillation, and this involves simulating ice-ocean-atmosphere interaction, and sea-ice changes in the Arctic; these issues are specifically called out in the DRI. The dynamics we are focusing on, beginning with tropopause polar vortices and their role in the evolution of Arctic surface pressure anomalies, sea ice distributions and evolution, and ultimately the AO, are significant multiscale dynamical processes, which ultimately affect climate. Finally, we appreciate the Navy's interest and need in next-generation global NWP systems and longer-time-scale prediction capability. We are working with Dr. James Doyle of the Naval Research Laboratory (NRL) to communicate how MPAS and MPAS-CESM may be applicable to Navy relevant research.

APPROACH

This study evaluates the performance of MPAS by examining a multi-scale feature that is common to the Arctic: Tropopause polar vortices (TPVs). TPVs are commonly observed tropopause-based vortices that originate in higher latitudes. TPVs are important to lower latitude predictability, because they are precursors to development of surface cyclones (Hakim and Canavan 2005; Cavallo and Hakim 2009; Cavallo and Hakim 2010). Yet, very little is known about how TPVs are linked with lower latitudes or their role in longer-term predictability. Higher latitude regions are a unique environment for growth and longevity of TPVs due to their relative position poleward of the polar jet stream and limited heat and moisture. Spatial scales of TPVs range as high as $\sim$1000 km and lifetimes can exceed 1 month (Cavallo and Hakim 2013). Lifetimes can be particularly long over the Arctic Ocean during summer months when the polar jet stream has a relatively weak influence (Cavallo and Hakim 2012). Given their longevity in the Arctic and their active role in surface cyclone formation and growth, we hypothesized that TPVs are an important component of longer-term prediction, and hence the predictability of sea ice.

The first portion of this study shows support that prediction beyond one week depends on the capability of numerical weather prediction models to accurately depict Rossby wave breaking events. Good prediction of Rossby wave breaking is necessary to accurately predict low-level atmospheric circulation over the Arctic Ocean. Thus, accurate prediction of sea ice depends on the predictability of Rossby wave breaking events. Fig. 1 illustrates our hypothesis with a conceptual model for the potential contribution of TPVs to Rossby wave

breaking, which comprises a feedback between TPVs, the arctic jet stream, the polar and subtropical jet streams, surface cyclones, and Rossby waves. Meridional extrusions of the polar jet stream are signatures of Rossby waves, and are centered about the strongest thermal gradients on the tropopause (Rossby et al. 1939). We believe that given the fact that TPVs encompass a coherent circulation anomaly of $\sim$20 m s^{-1} on average, the arctic jet (noted by a dotted purple circle) is a circulation feature associated with a TPV. Shapiro et al. (1987) first noted the presence of an arctic jet stream that is located on a tropopause fold that surrounds a so-called "polar vortex" with synoptic or sub-synoptic-scale spatial scales in the upper-troposphere. They furthermore noted that the location of this polar vortex was highly variable in the case they examined, moving between the high Canadian Arctic and midlatitudes of North America. Dotted lines in Fig. 1 illustrate our conceptual model of how the arctic jet stream interacts with lower latitude jet streams over time. Time=1 reflects the subtropical, polar, and arctic jets with a lower latitude heat source and an initially zonal flow and isolated TPV. Time=2 shows enhancement of wave growth in the presence of the arctic jet, which is a new factor being introduced by the proposed study. Time=3 illustrates the implication of introducing the arctic jet stream, where it is more likely for wave breaking to occur. If a wave breaks, TPVs will once again become isolated from the polar and subtropical jet streams, where they await the next wave interaction. PI Cavallo has previously shown that when a TPV is isolated from the polar jet, it intensifies through diabatic processes (Cavallo and Hakim 2010). This finding will be expanded in the proposed study by investigating whether diabatic processes significantly control the strength of the arctic jet by radiative processes associated with water vapor anomalies and clouds. Foundational knowledge for this hypothesis is described in the following sections.

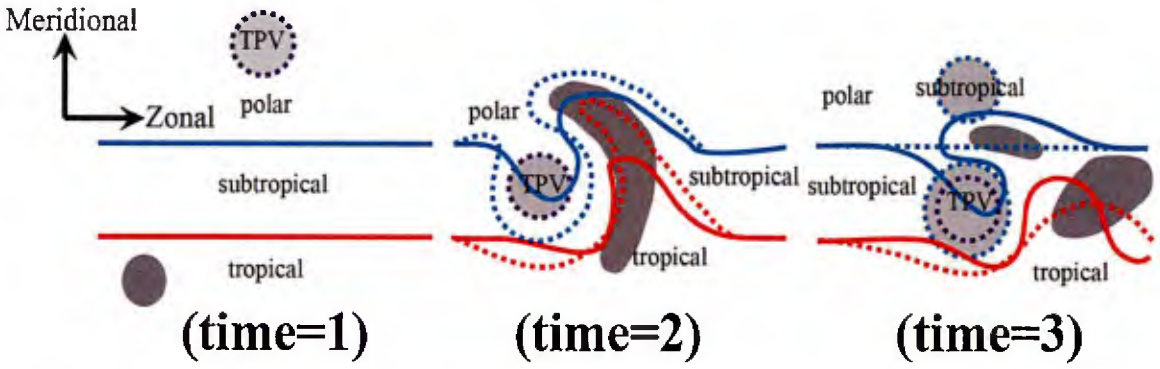

FIG. 1. ***TPVs and Rossby waves interact.*** *A schematic representation of the tropopause for a baroclinic wave during the early (Time= 1), developing (Time= 2), and mature (Time= 3) stages with arctic, polar, and subtropical jets. Contours representing the subtropical, polar, and arctic tropopause are denoted by the red, blue, and magenta lines, respectively with corresponding air masses labeled. Solid contours represent the evolution in the absence of an arctic jet, while dashed contours represent those contours only in the presence of an arctic jet. Regions of anomalous potential vorticity (PV) creation (destruction) in the presence of the arctic jet are shaded light (dark) gray.*

Model for Prediction Across Scales (MPAS)

The atmospheric component of MPAS was developed by the National Center for Atmospheric Research (NCAR) and solves the fully compressible nonhydrostatic equations using finite-volume numerics discretized on centroidal Voronoi (nominally hexagonal) meshes using C-grid staggering of the prognostic variables based on the work of Thuburn et al. (2009) and Ringler et al. (2010). The mesh configurations developed for this study are depicted in Fig. 2. We have chosen three different configurations in order to isolate the predictive benefits of having a smooth transition in horizontal resolution, and to further isolate the significance of remote forcings (such as upstream convection) on the prediction of Arctic cyclones.

The approach we are using to solve the nonhydrostatic equations can be considered an extension of existing techniques used in nonhydrostatic models to the horizontal Voronoi mesh; these techniques are used in the Advanced Research Weather Research and Forecasting (WRF-ARW) model, COAMPS, ARPS, etc. By using established techniques, MPAS leverages existing state-of-the-art technology, and preliminary tests show that MPAS will give solutions as accurate as WRF-ARW and similar models at both hydrostatic and nonhydrostatic scales (Skamarock et al. 2012). These techniques represent the state-of-the-art in mesoscale and cloud-scale modeling.

The quasi-uniform centroidal Voronoi meshes used within MPAS are similar to the icosahedral (hexagonal) meshes such as that used in other nonhydrostatic icosahedral atmospheric model, for example NICAM (Satoh et al. 2008). These meshes provide nearly uniform resolution over the globe and allow for good scaling performance on massively parallel architectures. MPAS represents, however, the first C-grid discretization on the sphere (normal velocities on the cell faces are prognosed, as opposed to solving for cell-centered velocities on the A-grid), and as such retains the accuracy of mesoscale and cloud-scale models (e.g., ARW, COAMPS, etc) that precede it.

In contrast to the MPAS centrical Voronoi mesh, global atmospheric models have typically employed latitude-longitude grids. Solvers employed on these meshes need special treatment in the polar regions that inhibit scaling on parallel computing architectures, or, in the case of spherical-transform based models, require Legendre transforms that do not scale well.

The centroidal Voronoi meshes also allow for local refinement, and the variable-resolution horizontal mesh takes advantage of the unstructured-mesh capabilities of the MPAS nonhydrostatic solver. The variable-resolution meshes are generated such that there is a gradual change in mesh density from the coarse to the high resolution regions, and as such allow for much more flexible mesh refinement capabilities than approaches using a remapping of a structured mesh. The smooth mesh transitions we use in MPAS stand in contrast to the abrupt mesh transitions used in traditional 2-way nested models such as WRF-ARW or in mesh refinement achieved directly through cell division using rectangles or triangles. We

believe the smooth mesh transition will ameliorate many of the difficulties associated with traditional nesting approaches as indicated by the recent results from Co-PI Skamarock and collaborators using the shallow water equations (Ringler et al. 2011).

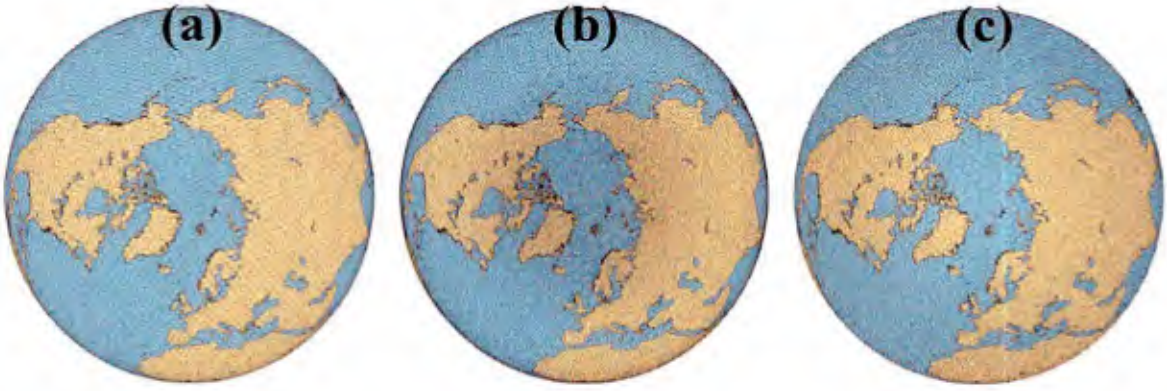

FIG. 2. ***MPAS is a global model that allows for a smooth grid transition in regions of interest.*** *Schematic of the MPAS C-grid horizontal discretizations that have been implemented for the current study. Comparisons are performed with a (a) uniform mesh containing nearly equal cell spacing globally, (b) and arctic-refined variable resolution mesh where cell spacing varies from ~30-km over the Arctic Ocean to ~60-km in lower latitudes, and (c) a midlatitude-refined variable resolution mesh where cell spacing varies from ~30-km over midlatitude regions and ~60-km over the Arctic region.*

A MULTI-SCALE APPLICATION—TROPOPAUSE POLAR VORTICES (TPVs)

This study focuses on identifying mechanisms that enhance predictability of physical and dynamical processes in polar regions, which are relatively weak in comparison to lower latitudes (Jung and Co-authors 2013). Sea ice and TPVs are unique factors of significance in the north polar region, most critical to our understanding and likely to be co-dependent. Prior studies have established the importance of synoptic-scale cyclones to the Earth's climate system, particularly for their role in transporting heat, momentum and moisture from lower-latitudes to the extratropics (e.g., Trenberth and Stepaniak 2003; Eckhardt et al. 2004; Schneider et al. 2006; Boutle et al. 2011). Tropopause dynamics are known to be important for subsequent surface cyclone development (e.g., Eliassen and Kleinschmidt 1957) and predictability. TPVs are critical to improving predictability because they are always associated with an upper-level PV anomaly, which is a necessary feature for type B surface cyclogenesis (e.g., Petterssen and Smebye 1971). Surface cyclones can accelerate sea ice loss, as observed in the summer of 2012 when an exceptionally strong cyclone developed over the Arctic Ocean (e.g., Simmonds and Rudeva 2012; Parkinson and Comiso 2013; Kriegsmann and Brümmer 2014; Zhang et al. 2013).

Diabatic processes govern TPV maintenance (Cavallo and Hakim 2009; Cavallo and

Hakim 2010); longwave radiative effects associated with water vapor anomalies are crucially necessary for TPV's intensification (Cavallo and Hakim 2012; Cavallo and Hakim 2013). These studies show that TPV intensification is most likely to occur at locations where temperatures are relatively cool and latent heating rates are limited, conditions most common in higher latitudes and over land or sea ice. The proposed study will address knowledge regarding the role and feedbacks between TPVs and sea ice, and about the roles of radiation and latent heating in intensifying and weakening TPVs in this process (Cavallo and Hakim 2010). If greater areas of open water increase upward sensible and latent heat fluxes into the atmosphere, they may increase the potential for latent heating to weaken TPVs. On the other hand, areas of open water located adjacent to sea ice or land areas increase the lower-level horizontal temperature gradients that promote surface cyclone development (e.g., Eady 1949).

TPVs tend to exhibit particularly long lifetimes over the Arctic Ocean during the summer months when the polar jet stream has a relatively small influence (Cavallo and Hakim 2012). A major focus of this study has been on evaluating the MPAS performance for a single TPV that remained quasi-stationary over the Arctic Ocean for several months during the summer of 2006. This particular TPV exerts a large impact on the mean summer atmospheric circulation, as evident in anomalously low 500 hPa geopotential heights from the NCEP Climate Forecast System Reanalysis (CFSR)(Saha and collaborators 2010) climatology during the months of June, July, and August (JJA)(Fig. 3a). In contrast, cyclonic TPVs are largely absent during the summer of 2007, which is reflected in the anomalously high 500 hPa geopotential heights over much of the Arctic Ocean during JJA (Fig. 3b). In these cases, the TPV mean circulations extend to the surface (not shown), where anomalously high (low) sea ice concentrations were observed during the summer of 2006 (2007) (Fig. 3c). Aided by the geography of the Arctic, cyclonic (anticyclonic) low-level circulation anomalies tend to increase (decrease) sea ice concentrations by flow in and out of the Arctic Ocean through the Bering and Fram Straits (e.g., Rigor et al. 2002).

Given the long lifetimes of some TPVs and their links to surface anomalies and Rossby wave breaking, we believe they may play a role in longer-term sea-ice anomalies. Reductions in sea ice have occurred much more rapidly than projections from global climate models (GCMs; e.g., Holland et al. 2006; Stroeve et al. 2007). Although many factors may contribute to this rapid sea ice decline, Ogi and Wallace (2007) noted that years with anomalously low (high) September sea ice extent are often preceded by anticyclonic (cyclonic) sea level pressure (SLP) anomalies over the Arctic Ocean. Serreze and Barrett (2008) showed that summer SLP anomalies over the Arctic extend to the 500 hPa level, and can broadly be linked to the phase of the AO. Sea ice movement has been observed to closely follow the lower level atmospheric circulation patterns (Rigor et al. 2002), consistent with estimates of a net surface forcing from the atmosphere toward the ocean during the summer months due to relatively high solar heating rates (Serreze et al. 2007). During the summer months when TPVs have longer lifetimes over the Arctic Ocean, their potential impact on the mean

atmospheric flow is greater than the winter and their associated anomalies are more likely to project with phases of the AO.

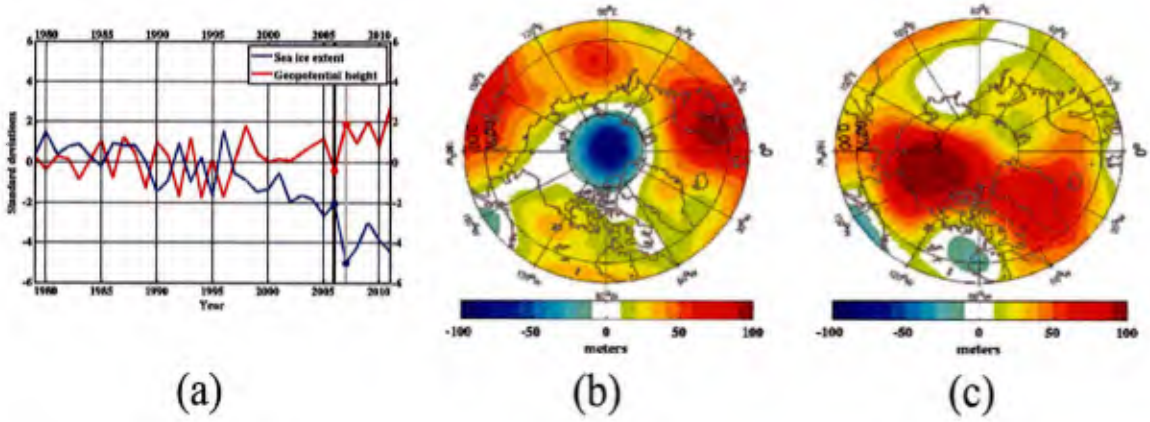

FIG. 3. ***Summer seasons with lower (higher) sea ice extent correlate to higher (lower) 500 hPa heights over the Arctic and a negative (positive) Arctic Oscillation pattern.*** *Anomalies in 500 hPa geopotential heights averaged over June, July, and August (JJA) during (a) 2006 and (b) 2007 with respect to climatologies from 1979-2010. The contour interval is 10 meters. (c) Time series of the standardized anomalies in JJA geopotential height (red) and September minimum sea ice extent (blue) with respect to climatologies from 1979-2000. The dark (light) gray vertical lines correspond to the year 2006 (2007), and the red (blue) dots are the values of geopotential height (sea ice extent) at the corresponding years.*

SHORT TIMESCALE VARIABILITY IN ARCTIC SEA ICE

To quantify changes in sea ice, we use daily sea ice extent (SIE) from the National Snow and Ice Data Center (NSIDC) Sea Ice Index (Fetterer et al. 2002). ΔSIE is the sum of the daily change in SIE from the previous 3 days. Moving 3-d sums of ΔSIE are spectrally filtered using a high-bandpass cutoff period of 18 days to isolate the short timescale variability are considered very rapid sea ice loss events (VRILEs). Extremes are treated as the tail of the distribution of SIE loss, here the lowest 5th-percentile in ΔSIE. We apply a high bandpass Butterworth filter with a cutoff frequency of 6.43×10^{-7} Hz (or a period of 18 days) to retain only the high frequency variability that is significant with respect to the 95% red noise spectrum (Fig. 4d). The days that correspond to the top 5th percentile are then used to define VRILEs. Occurrences of VRILEs on consecutive days are not eliminated, but are recognized as possibly being related to the same physical feature, such as a long-lived surface cyclone. To account for these occurrences, we reduce the VRILEs into a subset referred to as "Unique VRILEs", where any series of VRILEs identified on adjacent days are counted as a single event, with the date corresponding to the last day in the series.

Global climate model projections from the Community Earth System Model - Large Ensemble (CESM-LE)(Kay et al. 2015) show increasing Arctic ΔSIE variability as the climate warms, especially at timescales of at least one week (Fig. 4a). CESM-LE Arctic ΔSIE variability is only significant for periods of over 50 days in both present and future scenarios, indicating from this modeling perspective that VRILEs may not be a significant contribution to ΔSIE. However, observations show that Arctic ΔSIE variability is also significant for periods of about 15 days or less (Fig. 4b), implying that the CESM-LE, and potentially other climate models, are not representing the physical processes that produce the variability at weather timescales. Furthermore, observed atmospheric variability from intraseasonal variations such as the Arctic Oscillation (AO) and North Atlantic Oscillation (NAO) are significant at timescales of as short as one week (not shown), and since ΔSIE is in part associated with these patterns of atmospheric variability, CESM-LE may also not be representing the full range of impacts from them. The observation shown here that ΔSIE variability is significant at timescales of 15 days or less motivates the use of MPAS-CESM since the high-resolution atmosphere can more accurately represent these shorter timescales that are important for the interactions between TPVs, Arctic cyclones, and sea ice loss. Thus we hypothesize that accurately simulating the strength of synoptic weather, such as Arctic cyclones, is a key factor in accurately predicting sea ice loss due to the atmosphere-ice feedback.

RESULTS

In August 2006, there was an event in which the long-lived TPV moved over the sea ice margin (SIM) in the North Atlantic near Svalbard, Norway, inducing a strong surface cyclone (Fig. 5a). As an illustration of a primary deliverable directly from this project, MPAS-CESM successfully simulated the TPV and surface cyclone (Fig. 5b). Passive microwave satellite radiometry images following this event revealed a large and newly-developed ice-free region at the location of the cyclone (Fig. 5c), and the feedback between the atmosphere and sea ice motion is clearly evident in the MPAS-CESM simulation (Fig. 5d). A particular case is chosen for evaluation that incorporates the multi-scale aspects of atmosphere, ocean, and sea ice feedbacks. This case consists of a single TPV with an 86-day lifetime (Fig. 6a). The long lifetime results in a negative 500 hPa geopotential height anomaly during the entire warm season of 2006, centered over the central Arctic Ocean (Fig. 6b), that projects onto the Arctic Oscillation (Fig. 6c). Below we summarize the results leading up to the capability illustrated above of the coupled atmosphere-ocean-land-sea ice modeling system MPAS-CESM in performing medium to long range weather prediction (week - months) focusing on the Arctic region.

A hierarchical modeling approach begins with development and testing of the nonhydrostatic atmospheric component model, which we refer to as MPAS-A. The second portion of this research combines MPAS-A with the fully coupled Community Earth-system model

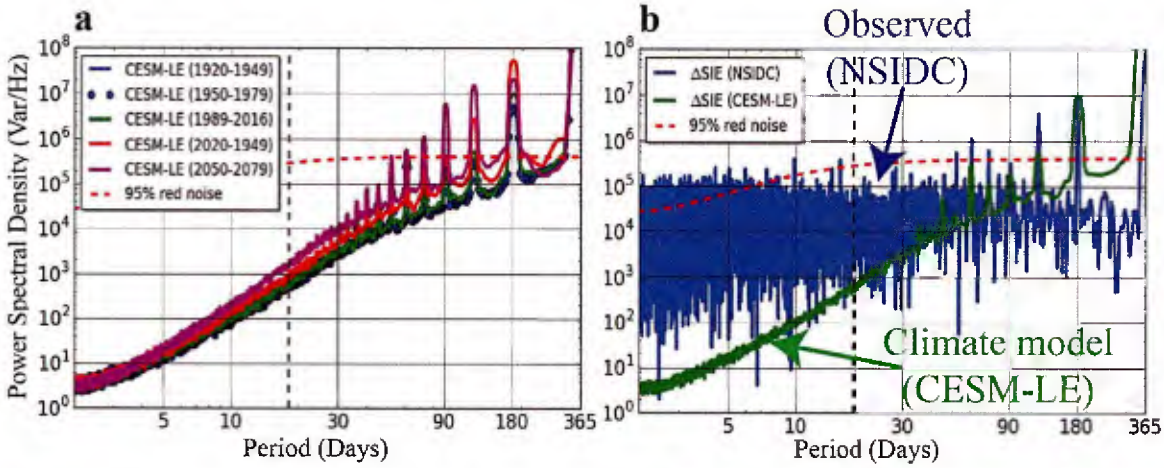

FIG. 4. ***There is signifcant sea ice variability at high frequencies (weather timescales) that are not represented in climate models.*** *ΔSIE Power spectral density (PSD) (a) in 30-yr periods from CESM-LE projections for 1920-1949 (blue), 1950-1979 (orange), 1989-2016 (green), 2020-2049 (red), and 2050-2079 (magenta) and (b) CESM-LE projection of the near present day equivalent (1989-2016 period; green) comparison to observations from the NSIDC sea ice index (1979-2017; blue). The 95% confidence interval from the theoretical red noise spectrum (dashed red) is also shown, and thus PSD values above this dashed red line indicate statistically significant ΔSIE variability. Units of PSD here is Variance Hz^{-1}. In (b), the green curve is bounded by the 0.05-99.5 percentile (p=0.01) bootstrap resampled 1000 times with the mean from the 30 members of the CESM-LE. The vertical dashed black line denotes the 18 day cutoff period used in the high bandpass filter to retain the weather timescales.*

(CESM), which we refer to as MPAS-CESM. This modeling configuration is now available to the general community through the National Center for Atmospheric Research (NCAR) as part of the CESM dynamical core options. Results are summarized here in the case of the long-lived (86-day lifetime) TPV over the Arctic Ocean during the summer of 2006 described above. Table 1 summarizes a description of the tasks taken to achieve the goals of this study.

Atmosphere only

We first analyze the performance of an MPAS-A ensemble for the 2006 TPV (Task T1 in Table 1). Ensemble members vary by mesh configuration and physics parameterizations, but all consist of the same dynamical core. Ensemble forecasts are initialized weekly beginning after TPV genesis. The composite results for all experiments show that TPV track forecasts diverge with 7-d forecast lead times on average (Fig. 7a). TPV intensity forecasts in the MPAS-A ensemble quickly diverge from observations immediately, and we find there is considerable sensitivity to the mesh spacing near the TPV (not shown). Regardless of the

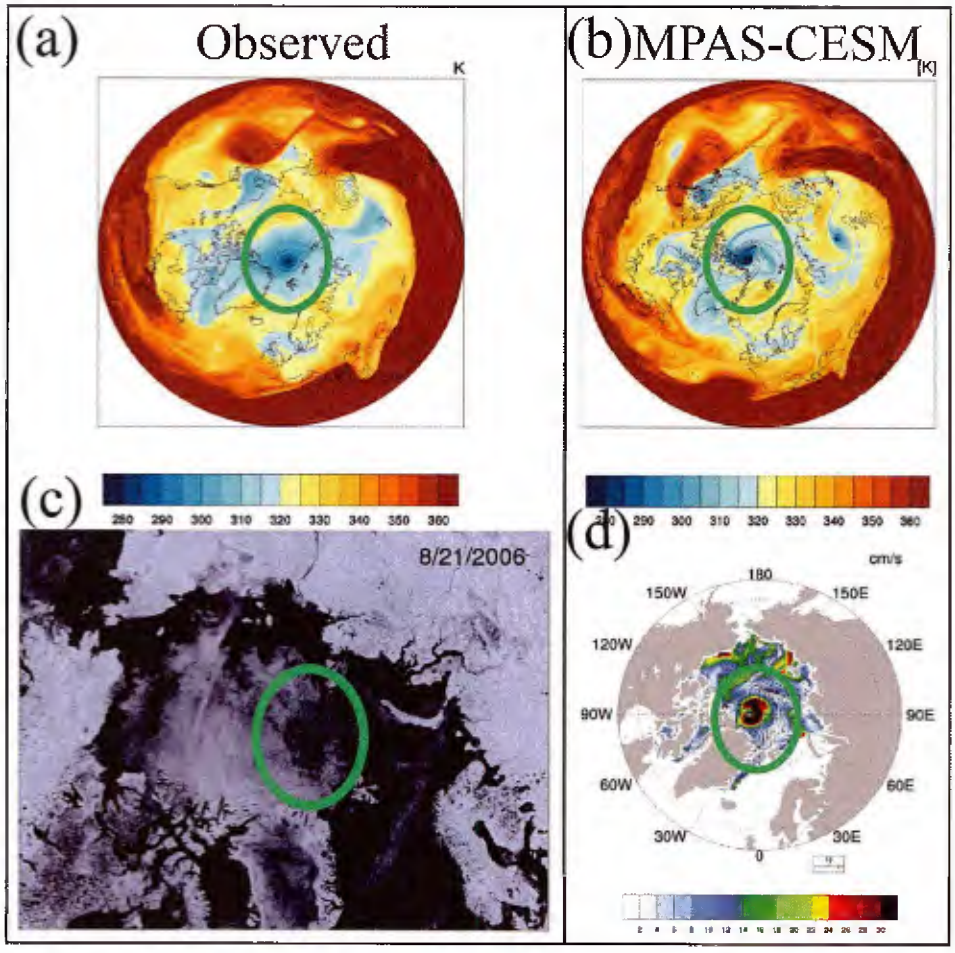

FIG. 5. **(a),(c) Observations vs. (b),(d) numerical modeling simulation of a hole in Arctic sea ice underneath an Arctic cyclone and tropopause polar vortex.** (a)-(b) Potential temperature on the dynamic tropopause (colors; color interval 5 K) and sea level pressure (black contours; contour interval 4 hPa; only values at or below 1004 hPa are shown) 00 UTC 21 August 2006, (c) sea ice concentration from passive microwave satellite radiometry composited over 21 August 2006, and (d) modeled sea ice velocity (cm s^{-1}). The green circle highlights a region of sea ice loss, evident by satellite observations (c) under an observationally-based model analysis of a TPV and Arctic cyclone in (a). The dynamic tropopause is the 2 PVU surface, where 1 PVU = 10^6 K m^2 kg^{-1} s^{-1}. The model simulations in (b) and (d) are from the MPAS-CESM configuration described in this report.

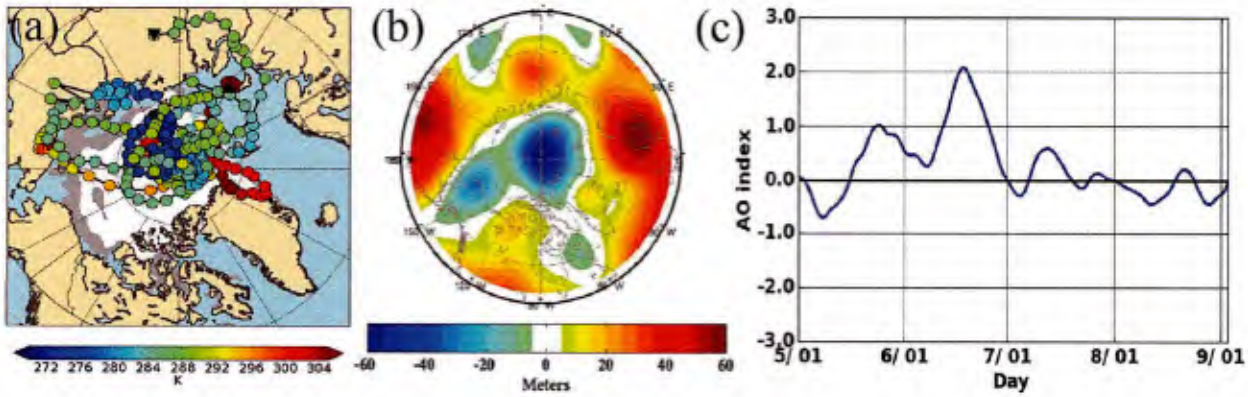

FIG. 6. ***The negative 500 hPa height anomaly over the Arctic and negative AO pattern in the summer season of 2006 are associated with a single, long-lived TPV.*** *(a) Vortex tracks with vortex intensity (colors) of a unique TPV during June-August 2006 from ERA-interim analyses (Dee et al. 2011). (b) Mean 2006 June-August 500 hPa geopotential height anomalies from NCEP/NCAR Reanalyses (Kalnay and collaborators 1996). (c) 10-d running mean of the Arctic Oscillation (AO) index from May - September 2006 (Data source: NOAA Climate Prediction Center).*

TABLE 1. Summary of major tasks completed.

Task number	Major task	Descriptions
T1	MPAS-A warm season experiments	(i) Ensemble experiments for Summer 2006 (ii) Summer 2007 analysis (iii) Comparison with TIGGE ensemble
T2	MPAS-A seasonal sensitivity experiments	(i) MPAS evaluation vs. ECMWF forecast "bust" case
T3	MPAS-CESM configuration	(i) Couple MPAS-A (nonhyrdostatic) with CESM components (ii) Spin-up ocean and sea ice modeling components
T4	MPAS-CESM sea ice experiments	(i) Atmosphere only, CAM physics case study experiment. (ii) Hierarchical coupling with ocean, sea ice modeling components

physics parameterization, intensity is best predicted for a mesh with local refinement over

the Arctic (Recall Fig. 2b). Conversely, the least skillful track forecasts occur when the local refinement region is in midlatitude regions (Recall Fig. 2c). This suggests that accurately resolving the TPV is more critical to forecasting vortex track than resolving midlatitude convection.

To extend the generality of these results, and to evaluate whether results are unique to MPAS-A, TPV intensity forecasts from the THORPEX Interactive Grand Global Ensemble (TIGGE; Bougeault et al. 2010) are analyzed. TIGGE consists of ensemble forecast data from 10 global numerical weather prediction centers, and is freely available for scientific research. This includes forecasts from the operational European Center for Medium Range Forecasting (ECMWF) integrated Forecasting System (IFS), consisting of a high-resolution deterministic forecast member and 51-ensemble members (Buizza et al. 2007). The composite forecast results from the 2006 TPV case in TIGGE indicate that intensity forecasts diverge with 4-6 day forecast lead times (Fig. 7b). Furthermore, all ensemble members under-forecast TPV intensity of the 2006 TPV. To further generalize whether systematic forecast biases exist in TPV intensity, intensifying TPVs in TIGGE forecasts between October 2006 and June 2005 with $\geq$5-day lifetimes are compared to ERA-interim analyses; these conditions yield 35 total cases. Results indicate that in 89% of the cases, TIGGE members under-forecasts 1-day changes in TPV intensity (Fig. 7c). Therefore, we conclude that modern operational forecast models tend to under-predict the strength of long-lived TPVs. This suggests that there is a missing key process in current operational models that inhibits an accurate representation of TPV evolution. We next explore sensitivities in TPVs in order to quantify their potential impact on Arctic cyclones and sea ice.

Object-based idealized experiments

To evaluate seasonal sensitivity, we next identify a case on 10 October 2010 where verification of extended range forecasts is particularly poor (Task 2 of Table 1). The atmospheric pattern on 10 October 2010 corresponds to a transition from a positive to a negative NAO pattern. In order to test the impact that a TPV has on subsequent forecast evolution, we developed a method to numerically weaken a TPV based on the known physical processes previously identified by Cavallo and Hakim (2013) as the primary intensification process of TPVs. This method allows us to bypass vortex removal methods, which have limitations due to necessary assumptions that must be made in order to replace a vortex with a balanced atmospheric state (e.g., Davis and Emanuel 1991; Demirtas and Thorpe 1999; Browning 1999). In particular, we use information about the longwave radiative cooling rates (Fig. 8a) that are associated with the longwave radiative response to water vapor (Cavallo and Hakim 2013). An additional forcing term is added within the model integration that follows the vortex by identifying a closed contour of tropopause potential temperature that surrounds the TPV at the forecast initialization time, and then applying thermodynamic heating in all columns within that region everywhere in the troposphere (Fig. 8b). This

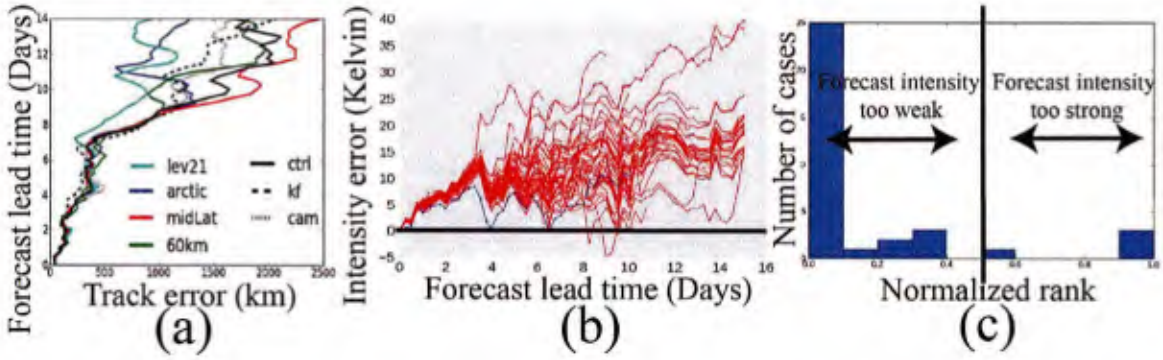

FIG. 7. ***TPV tracks are predictable for about a week, while intensity forecasts exert an immediate bias.*** *(a) Composite ensemble MPAS TPV track error (x-axis) vs. forecast lead time (y-axis) for the 2006 warm season long-lived TPV. (b) Ensemble TIGGE intensity error (y-axis) vs. forecast lead time (x-axis) for the 2007 warm season long-lived TPV. (c) Rank histogram of TPV intensity in the TIGGE ensemble. Error is the difference between the forecasts and ERA-interim reanalysis values (Forecast minus reanalysis). (c) Rank histogram of TPV 5-d intensity error in TIGGE for all TPVs that are intensifying at analysis time for the time period October 2006 - June 2015. In (b), intensity is defined as the minimum potential temperature on the 2-PVU dynamic tropopause in the vortex. Thus positive (negative) values in (b) imply the forecast vortex is weaker (stronger) than the estimate from reanalysis data. The blue line in (b) represents the ensemble member with the highest resolution. In (c), a lower (higher) normalized rank corresponds to an ensemble member with a forecast vortex that is weaker (stronger) than the estimate from reanalysis data.*

thermodynamic heating is designed to oppose the longwave cooling responsible for the TPV intensification. After 60-h of model integration, the TPV is completely damped (Fig. 8c).

Using this method to weaken a TPV, a sensitivity experiment is designed to test the impact of TPV intensity on downstream forecasts. The control forecast simulation is an MPAS-A simulation with initial and boundary conditions from ERA-interim, initialized 00 UTC 4 October 2010. An experiment simulation is performed where the only difference from the control simulation is that the TPV is dampened as described above. Differences reveal that the TPV impact spreads downstream into the North Atlantic through eastern North America, and also into the North Pacific through Siberia, *concurrently* (Fig. 9a,b). Note that the error that reaches the polar jet stream from the North Pacific pathway through Siberia would appear as an upstream bias at nearly the same time as the downstream bias reaches the North Atlantic. The paths that these differences evolve on coincide with the pathways that TPVs most often take as they are transported out of the Arctic and into lower latitudes (Fig. 9c). This demonstrates that a TPV can have a substantial hemispheric impact from short to extended time scales in middle latitudes.

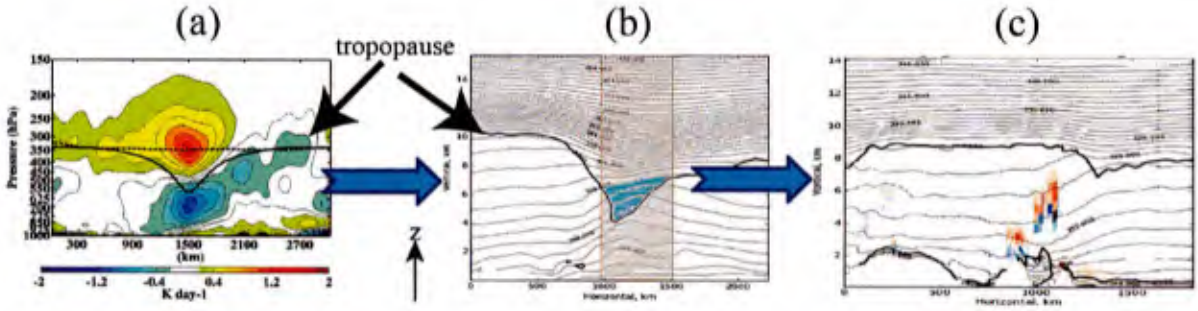

FIG. 8. ***Idealized experiments can be performed in MPAS-CESM that target object-based processes.*** *Cross sections (a) across composite TPVs with longwave radiative heating rate anomalies (Cavallo and Hakim 2010), (b), across a TPV over the Canadian Arctic on 4 October 2010 in MPAS, and (c) across a region where the TPV in (b) was damped in an MPAS forecast on 6 October 2010 at 12 UTC.*

Atmosphere, Ocean, and Sea Ice Couplings

One of the major achievements of this project is the development of a new numerical modeling tool for Arctic predictability studies to examine process-based hypotheses. This modeling system utilizes the following Earth-system component models within the CESM framework (Fig. 10), which are coupled using the CPL7 coupler with fluxes on the atmospheric grid. The modeling components include the POP2 (ocean model) on 1° Greenland tri-pole and 1 day coupling to atmosphere, CLM4 (land model) on 1° finite volume grid with 30 min coupling to atmosphere, CICE5 (sea ice model) on 1° Greenland tri-pole with 30 minute coupling to atmosphere, RTM (river model) with 3-hour coupling, the GLC land-ice model, and the WAV ocean wave model. We replace the CESM default Community Atmospheric Model (CAM) with the nonhydrostatic version of MPAS-A. The higher atmospheric resolution is clearly apparent in relative vorticity from our first simulation of the 2006 TPV (Fig. 11).

One of the remaining challenges of using an Earth-system model such as MPAS-CESM in "weather forecasting" mode (i.e., forecasts are initialized from a given analysis or reanalysis based on observations of the atmospheric state) is with regard to model spinup. Spinup is the modeling system's adjustment from initial conditions to its own climatological state, which for an atmosphere-only model, occurs on short time scales on the order of days (e.g., Rodwell and Palmer 2007). However, when including models that simulate slower processes at longer time scales, such as an ocean model, spinup is on the order of years. If we want to use a

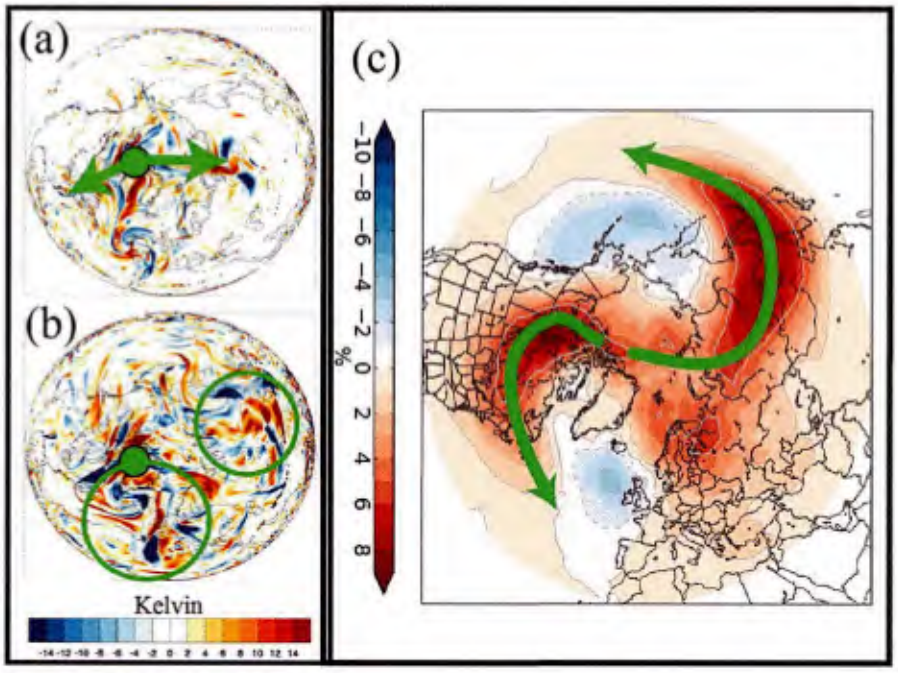

FIG. 9. ***Bias in TPV intensity spreads upstream and downstream into midlatitudes.*** *MPAS-A (a) 84-h and (b) 144-h forecast differences for an experiment where a TPV was damped during the first 48-h of integration. Forecasts are initialized 4 October 2010 at 00 UTC. (c) ERA-interim (1979-2015) winter TPV track density anomalies (colors) illustrated as the difference between winter and annual TPV probabilities at a given location. Green arrows correspond to the "pathways" of relatively dense TPV tracks in the winter. Green circles in (a) and (b) denote the location where a TPV was damped in the experiment.*

model to learn about physical processes, it is important that the model tendencies not be overshadowed by spinup (e.g., Cavallo et al. 2016). To account for this, we find an ensemble member from the Community Earth System Model Large Ensemble (CESM-LE; Kay et al. 2015) that is closest to an observed initial condition in a chosen metric. The CESM-LE consists of 30 simulations for the period 1920-2100, each with identical external radiative forcing, but beginning from slightly different initial conditions. Historical forcing was applied for 1920-2005 and representative concentration pathway 8.5 (RCP8.5) radiative forcing was used for 2006-2100. The CESM-LE uses the exact modeling components as our modeling system described here, except for the atmospheric component. Thus, by choosing a restart file from a particular ensemble member of the CESM-LE, we are able to begin simulations from an ocean model that is already spun-up. Then, the remaining spinup derives primarily from the atmospheric model, which is equivalent to the spinup from typical regional models that use a non-native analysis for initial conditions. This analog initial condition approach (e.g., Lorenz 1969) is most similar to a "Dynamic Analog Initialization" (Li et al. 2013), and we choose to initialize from an ensemble member that has the minimum difference in sea ice

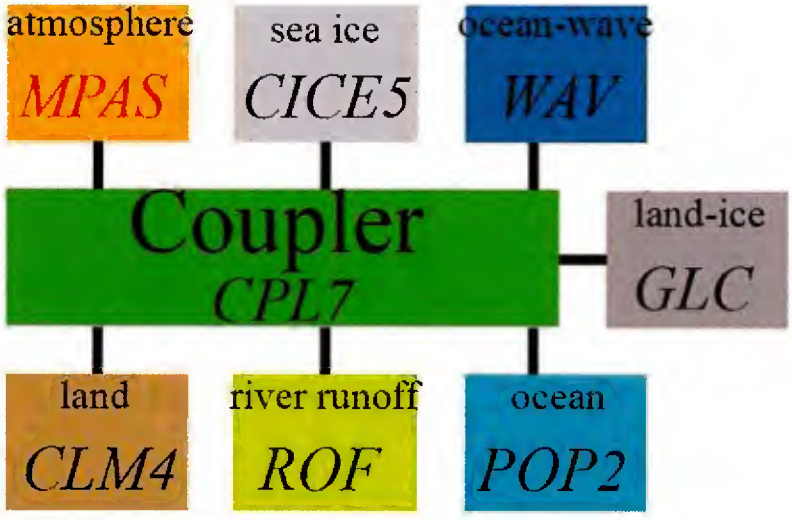

FIG. 10. ***MPAS-CESM is a fully-coupled Earth system model with a high-resolution nonhydrostatic atmospheric component.*** *Configuration of the MPAS-CESM. This fully coupled Earth System prediction system consists of seven geophysical models: atmosphere (MPAS-A nonhydrostatic), sea-ice (CICE5), land (CLM4), river-runoff (ROF), ocean (POP2), land-ice (GLC), and ocean-wave (WAV). A coupler (CPL7) coordinates the geophysics models time evolution and passes information between them.*

extent (SIE) at a given initialization time.

In testing the hypothesis that accurately simulating the strength of synoptic weather, such as Arctic cyclones, is a key factor in accurately predicting sea ice loss due to the atmosphere-ice feedback, we perform both real-data and idealized numerical simulations with the fully coupled version of MPAS-CESM. The real-data cases are in conjunction with the Study of Environmental Arctic Change (SEARCH) Sea Ice Outlook (SIO) forecasts of September Arctic sea ice extent. Using this analog initial condition approach, we test the impact on sea ice by uncertainties in atmospheric initial conditions by beginning SIO forecasts from slightly different atmospheric states using the deterministic Global Forecasting System (GFS) and Global Ensemble Forecast System (GEFS). The Great Arctic Cyclone of 2012 is strongly linked to an acceleration of sea ice loss. MPAS-CESM forecasts produce a pattern of strong Arctic cyclone activity and accelerated sea ice loss, in contrast to the CESM-LE, despite MPAS-CESM being initialized from CESM-LE (Fig. 12a). Without addressing biases in initial conditions, MPAS-CESM 2-month forecasts are quite competitive with the other SIO forecasts (Fig. 12b). For 2017 SIO forecasts, forecasts initialized with the deterministic GFS atmosphere, MPAS-CESM performs with the 2nd most skillful forecast of the 37 SIO forecast models (Fig. 12d). We furthermore discovered that the ensemble members initialized from GEFS were significantly worse, which we are now investigating. A noteworthy point about GEFS initial conditions is that they are derived from a coarser-resolution version of GFS.

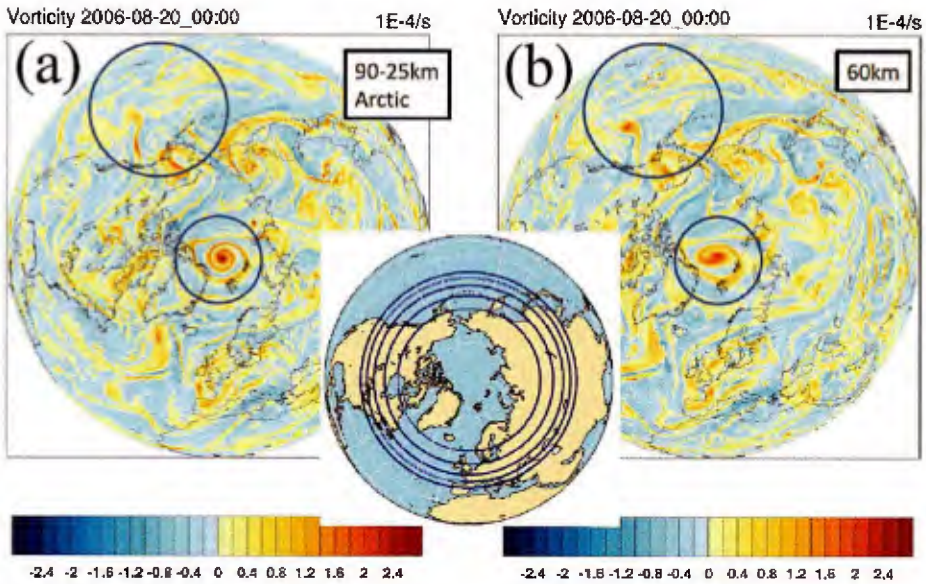

FIG. 11. ***The mesoscale structure within TPVs becomes apparent with higher atmospheric resolution.*** *500 hPa relative vorticity at forecast hour 120 from MPAS-CESM with (a) variable resolution with 25-km mesh spacing over the Arctic that smoothly transitions to 90-km spacing elsewhere, and (b) MPAS-CESM globally uniform 60-km mesh spacing. Forecasts are initialized 00 UTC 15 August 2006 from ERA-interim initial conditions.*

This is furthermore consistent with our hypothesis that it is important to represent smaller atmospheric scales in order to accurately predict TPVs, Arctic cyclones, and the resulting sea ice loss.

A summary of all idealized sensitivity experiments is listed in Table 2, and are based on a 2006 and 2007 MPAS-CESM month-long control run initialized 00 UTC 1 August. The trends in 2006 vs. 2007 SIE reflect the observed trends, namely with much lower SIE by mid September 2007 in comparison to 2006. Large sensitivity occurs when all 2006 TPVs poleward of 50°N latitude are artificially strengthened, resulting in substantially greater SIE (Fig. 13a). Recall this season consists of primarily one long-lived TPV over the central Arctic with a corresponding surface cyclone (Fig. 14a,c). The longevity is partially due to limited Rossby wave interaction, and the enhanced cloud-cover early in the season prevents solar radiation from reaching the surface, limiting early season thermodynamic sea ice melt. In 2007, a lack of early-season TPVs corresponds to anomalously low cloud cover and high sea ice melt near the Arctic Ocean coastlines during the months of June and July. However, Rossby wave interactions with TPVs are greater in 2007 since TPVs are located anomalously equatorward and closer to the polar jet stream. Combined with open waters over the Arctic Ocean near the coast, the pattern of high pressure shifts to a pattern of frequent storms when TPVs begin moving over the newly open water over the Arctic Ocean. The impact

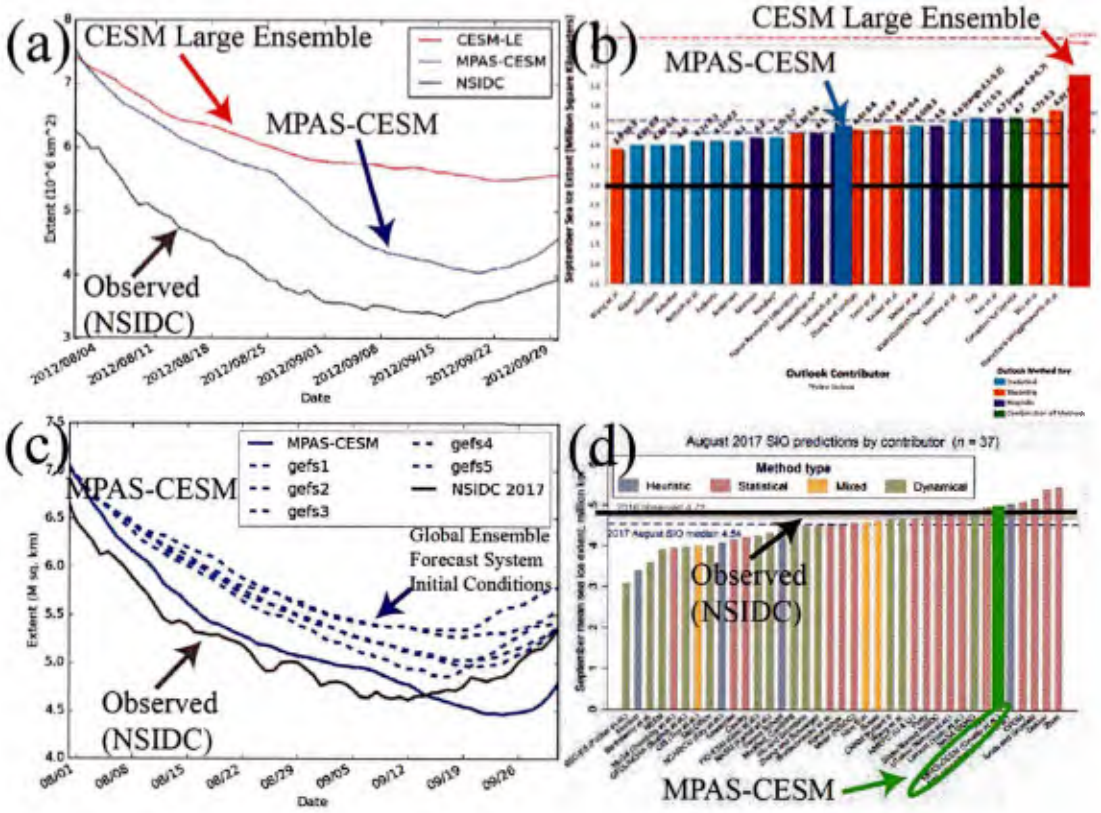

FIG. 12. ***MPAS-CESM produces competitive subseasonal-to-seasonal forecasts of September minimum sea ice extent.*** *MPAS-CESM Study of Environmental Arctic Change (SEARCH) Sea Ice Outlook (SIO) forecasts of September Arctic sea ice extent initialized 1 August (a)-(b) 2012 and (c)-(d) 2017 with a (a),(c) time series of sea ice extent (SIE) and (b),(d) ranking of mean September SIE in comparison to all other SEARCH SIO forecasts.*

of TPV strength and enhanced sea ice velocity is clearly illustrated as the 2006 TPV is strengthened by rates of -5 K day^{-1} (Fig. 14b,e) and -10 K day^{-1} (Fig. 14c,f). Furthermore, these sensitivity experiments show that localized TPV perturbations can impact zonal-mean momentum (Fig. 13b). For example, in the 2006 case, strengthening TPVs *equatorward* of 65°N increases Rossby wave activity, allowing the long-lived TPV to move out of the Arctic.

IMPACT/APPLICATIONS

The MPAS-CESM modeling configuration developed during this project is now available to the general community through the National Center for Atmospheric Research (NCAR) as part of the Community Earth System Model (CESM) dynamical core options: `https://ncar.ucar.edu/what-we-offer/models/model-prediction-across-scales-mpas`.

TABLE 2. *Summary of TPV modification sensitivity experiments. All simulations use fully-coupled MPAS-CESM for a 1-month forecast duration beginning 00 UTC 15 August of the respective year.*

Simulation title	Description
X2006	2006 Control
X2007	2007 Control
W2006_N65N	Warm (weaken) all 2006 TPVs poleward of 65°N latitude
C2006_N65N	Cool (strengthen) all 2006 TPVs poleward of 65°N latitude
C2006_N50N	Cool (strengthen) all 2006 TPVs poleward of 50°N latitude
C2006_S65N	Cool (strengthen) all 2006 TPVs equatorward of 65°N latitude
C2007_N65N	Cool (strengthen) all 2007 TPVs poleward of 65°N latitude
W2007_N65N	Warm (weaken) all 2007 TPVs poleward of 65°N latitude

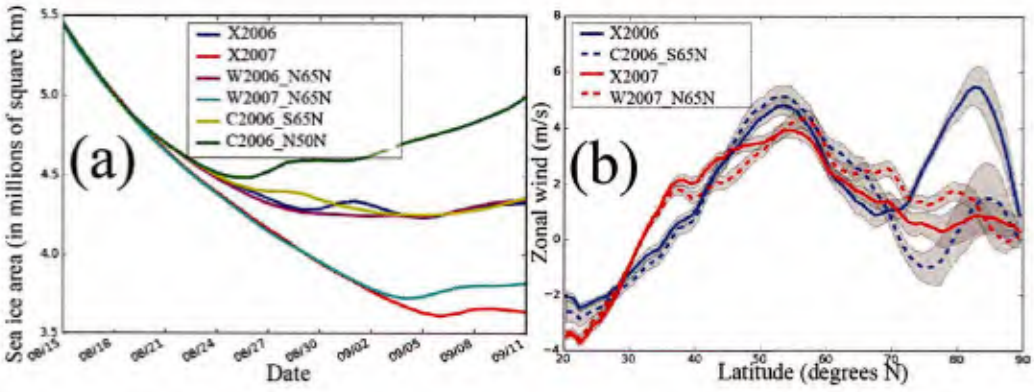

FIG. 13. ***Changes in TPV intensity significantly impacts the seasonal atmospheric pattern.*** *MPAS-CESM (a) time series of shifted sea ice extent ($\times 10^6$ km^2) and (b) 850 hPa zonal mean wind as a function of latitude for the TPV modification sensitivity experiments. Values for each of the curves in (a) are shifted by a constant so that they begin on 15 August with the same values, and thus curves reflect trends, and not the actual sea ice extents. Shadings in (b) are the 95% bootstrap confidence intervals on the mean from 6-hourly samples. Refer to Table 2 for a description of the experiments.*

TRANSITIONS

None.

RELATED PROJECTS

This research helped motivate ONR Department Research Initiative (DRI) "Overcoming the Barrier to Extended Range Prediction over the Arctic." The aim is to enhance the

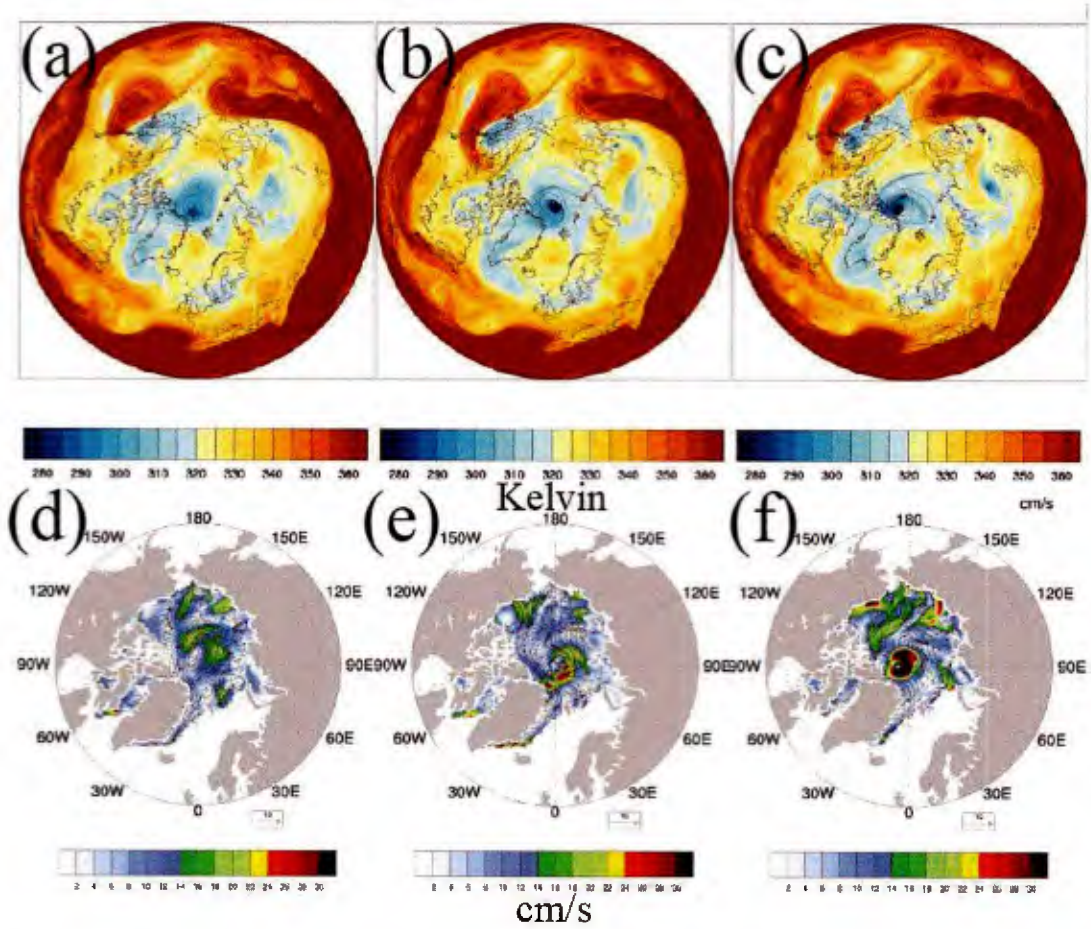

FIG. 14. ***Stronger TPVs are associated with faster sea ice flow.*** *MPAS-CESM (a)-(c) tropopause potential temperature (colors; units of Kelvin) and sea level pressure (contours; units of hPa; only contoured for values less than 1000 hPa) and (d)-(f) sea ice velocity magnitude (colors; units of cm s^{-1}) and motion vectors (arrows) for the (a),(d) X2006, (b),(e) C2006_N50N with -5 K cooling, and (c), (f) C2006_N50N with -10 K cooling simulations at forecast hour 120.*

understanding of dynamics of Arctic cyclones and their relationship to the tropopause polar vortex (TPV), and will involve a large-scale aircraft campaign in the Arctic.

REFERENCES

Bougeault, P., et al., 2010: The THORPEX Interactive Grand Global Ensemble. *Bull. Amer. Meteor. Soc.*, **91 (8)**, 1059–1072, doi:10.1175/2010BAMS2853.1.

Boutle, I. A., S. E. Belcher, and R. S. Plant, 2011: Moisture transport in midlatitude cyclones. *Quart. J. Roy. Meteor. Soc.*, **137 (655)**, 360–373.

Browning, K. A., 1999: Mesoscale aspects of extratropical cyclones: An observational perspective. *The life cycles of extratropical cyclones*, Springer, 265–283.

Buizza, R., J.-R. Bidlot, N. Wedi, M. Fuentes, M. Hamrud, G. Holt, and F. Vitart, 2007: The new ECMWF VAREPS (variable resolution ensemble prediction system). *Quart. J. Roy. Meteor. Soc.*, **133 (624)**, 681–695.

Cavallo, S. M., J. Berner, and C. Snyder, 2016: Diagnosing model error from time–averaged tendencies in the weather research and forecasting model. *Mon. Wea. Rev.*, **144 (2)**, 759–779.

Cavallo, S. M. and G. J. Hakim, 2009: Potential vorticity diagnosis of a tropopause polar cyclone. *Mon. Wea. Rev.*, **137 (4)**, 1358–1371.

Cavallo, S. M. and G. J. Hakim, 2010: The composite structure of tropopause polar cyclones from a mesoscale model. *Mon. Wea. Rev.*, **138 (10)**, 3840–3857, doi:10.1175/2010MWR3371.1.

Cavallo, S. M. and G. J. Hakim, 2012: Radiative impact on tropopause polar vortices over the arctic. *Mon. Wea. Rev.*, **140 (5)**, 1683–1702.

Cavallo, S. M. and G. J. Hakim, 2013: The physical mechanisms of tropopause polar cyclone intensity change. *J. Atmos. Sci.*, **70**, 3359–3373.

Davis, C. A. and K. A. Emanuel, 1991: Potential vorticity diagnostics of cyclogenesis. *Mon. Wea. Rev.*, **119 (8)**, 1929–1953.

Dee, D. P., et al., 2011: The ERA-Interim reanalysis: Configuration and performance of the data assimilation system. *Quart. J. Roy. Meteor. Soc.*, **137**, 553–597.

Demirtas, M. and A. J. Thorpe, 1999: Sensitivity of short-range weather forecasts to local potential vorticity modifications. *Mon. Wea. Rev.*, **127 (5)**, 922–939.

Eady, E. T., 1949: Long waves and cyclone waves. *Tellus*, **1**, 33–52.

Eckhardt, S., A. Stohl, H. Wernli, P. James, C. Forster, and N. Spichtinger, 2004: A 15-year climatology of warm conveyor belts. *J. Climate*, **17 (1)**, 218–237.

Eliassen, A. and E. Kleinschmidt, 1957: *Handbuch der Physik*, Vol. 48. Springer Verlag, 154 pp.

Fetterer, F., K. Knowles, W. Meier, and M. Savoie, 2002: Sea ice index. *Natl Snow and Ice Data Center, Boulder, CO) Available at* `http://nsidc.org/data/g02135`. *Accessed 21 January 2018.*

Hakim, G. J. and A. K. Canavan, 2005: Observed cyclone-anticyclone tropopause asymmetries. *J. Atmos. Sci.*, **62 (1)**, 231–240.

Holland, M. M., C. M. Bitz, and B. Tremblay, 2006: Future abrupt reductions in the summer Arctic sea ice. *Geophys. Res. Lett.*, **33 (L23503)**, doi:10.1029/2006GL028024.

Jung, T. and Co-authors, 2013: WWRP Polar Prediction Project science plan. Accessed: 2018-09-08, `https://www.polarprediction.net/fileadmin/user_upload/www.polarprediction.net/Home/Documents/Final_WWRP_PPP_Science_Plan.pdf`, accessed: 2018-09-08.

Kalnay, E. and collaborators, 1996: The NCEP/NCAR 40-year reanalysis project. *Bull. Amer. Meteor. Soc.*, **77**, 437–472.

Kay, J. E., et al., 2015: The Community Earth System Model (CESM) large ensemble project: A community resource for studying climate change in the presence of internal climate variability. *Bull. Amer. Meteor. Soc.*, **96**, 1333–1349.

Kriegsmann, A. and B. Brümmer, 2014: Cyclone impact on sea ice in the central Arctic Ocean: A statistical study. *The Cryosphere Discussions*, **7**, 1141–1176.

Li, S., X. Rong, Y. Liu, Z. Liu, and K. Fraedrich, 2013: Dynamic analogue initialization for ensemble forecasting. *Adv. Atmos. Sci.*, **30 (5)**, 1406.

Lorenz, E. N., 1969: Atmospheric predictability as revealed by naturally occurring analogues. *J. Atmos. Sci.*, **26 (4)**, 636–646.

Ogi, M. and J. M. Wallace, 2007: Summer minimum Arctic sea ice extent and the associated summer atmospheric circulation. *Geophys. Res. Lett.*, **34**, doi:10.1029/2007GL029897.

Parkinson, C. L. and J. C. Comiso, 2013: On the 2012 record low Arctic sea ice cover: Combined impact of preconditioning and an August storm. *Geophys. Res. Lett.*, **40 (4)**, 1356–1361, doi:10.1002/grl.50349.

Petterssen, S. and S. J. Smebye, 1971: On the development of extratropical cyclones. *Quart. J. Roy. Meteor. Soc.*, **97**, 457–482.

Rigor, I. G., J. M. Wallace, and R. L. Colony, 2002: Response of sea ice to the Arctic Oscillation. *J. Climate*, **15**, 2648–2663.

Ringler, T., D. Jacobsen, L. Ju, M. Gunzburger, M. Duda, and W. C. Skamarock, 2011: Exploring a multi-resolution modeling approach within the shallow-water equations. *Mon. Wea. Rev.*, **139 (11)**, 3348–3368.

Ringler, T., J. Thuburn, J. B. Klemp, and W. C. Skamarock, 2010: A unified approach to energy conservation and potential vorticity dynamics for arbitrarily–structured C–grids. *J. Comp. Phys.*, **229**, 3065–3090.

Rodwell, M. J. and T. N. Palmer, 2007: Using numerical weather prediction to assess climate models. *Quart. J. Roy. Meteor. Soc.*, **133**, 129–146.

Rossby, C.-G. et al., 1939: Relation between variations in the intensity of the zonal circulation of the atmosphere and the displacements of the semi-permanent centers of action. *J. Mar. Res.*, **2 (1)**, 38–55.

Saha, S. and collaborators, 2010: The NCEP climate forecast system reanalysis. *Bull. Amer. Meteor. Soc.*, **91**, 1015–1057.

Satoh, M., T. Masuno, H. Tomita, H. Miura, T. Nasuno, and S. Iga, 2008: Nonhydrostatic icosahedaral atmospheric model (NICAM) for global cloud resolving simulations. *J. Comp. Phys.*, **227**, 3486–3514.

Schneider, T., K. L. Smith, P. A. OGorman, and C. C. Walker, 2006: A climatology of tropospheric zonal-mean water vapor fields and fluxes in isentropic coordinates. *J. Climate*, **19 (22)**, 5918–5933.

Serreze, M. C. and A. P. Barrett, 2008: The summer cyclone maximum over the central Arctic ocean. *J. Climate*, **21 (5)**, 1048–1065, doi:10.1175/2007JCLI1810.1.

Serreze, M. C., A. P. Barrett, A. G. Slater, M. Steele, J. Zhang, and K. E. Trenberth, 2007: The large-scale energy budget of the Arctic. *J. Geophys. Res.*, **112 (D11122)**, doi:10.1029/2006JD008230.

Shapiro, M. A., T. Hampel, and A. J. Krueger, 1987: The arctic tropopause fold. *Mon. Wea. Rev.*, **115 (2)**, 444–454.

Simmonds, I. and I. Rudeva, 2012: The great Arctic cyclone of August 2012. *Geophys. Res. Lett.*, **39 (L23709)**, doi:10.1029/2012GL054259.

Skamarock, W. C., J. B. Klemp, M. G. Duda, L. Fowler, S. .-H. Park, and T. D. Ringler, 2012: A multi-scale nonhydrostatic atmospheric model using centroidal voronoi tesselations and C–grid staggering. *Mon. Wea. Rev.*, **140**, 3090–3105.

Stroeve, J., M. M. Holland, W. Meier, T. Scambos, and M. Serreze, 2007: Arctic sea ice decline: Faster than forecast. *Geophys. Res. Lett.*, **34 (9)**, doi:10.1029/2007GL029703.

Thuburn, J., T. Ringler, W. C. Skamarock, and J. B. Klemp, 2009: Numerical representation of geostrophic modes on arbitrarily structured C-grids. *J. Comp. Phys.*, **228**, 8321–8335.

Trenberth, K. E. and D. P. Stepaniak, 2003: Covariability of components of poleward atmospheric energy transports on seasonal and interannual time-scales. *J. Climate*, **16**, 36913705.

Zhang, J., R. Lindsay, A. Schweiger, and M. Steele, 2013: The impact of an intense summer cyclone on 2012 Arctic sea ice retreat. *Geophys. Res. Lett.*, **40 (4)**, 720–726, doi:10.1002/grl.50190.

PUBLICATIONS AND PROCEEDINGS

Cavallo, S. M., 2012a: Arctic weather or climate? Tropopause polar vortices, sea ice, and midlatitude cyclogenesis. *Invited seminar, The Weather-Climate Intersection: Advances and Challenges*, Boulder, CO, National Center for Atmospheric Research Advanced Study Program.

Cavallo, S. M., 2012b: Coherent vortices over the arctic: Their role in the predictability of our weather and what may change with reductions in Arctic sea ice. *Invited colloquium*, Marietta, GA, Southern Polytechnic State University.

Cavallo, S. M., 2016a: Diagnosing systematic numerical weather prediction model bias over the Antarctic from short-term forecast tendencies. *Invited lecture*, Zurich, Switzerland, Federal Office of Meteorology and Climatology/MeteoSwiss.

Cavallo, S. M., 2016b: Diagnosing systematic numerical weather prediction model bias over the Antarctic from short-term forecast tendencies. *Invited seminar*, Reading, UK, European Center for Medium Range Forecasting (ECMWF).

Cavallo, S. M., 2016c: Sensitivity of the midlatitude waveguide to the dynamics and observations of tropopause polar vortices. *Invited lecture*, Zurich, Switzerland, Swiss Federal Institute of Technology in Zurich (ETH).

Cavallo, S. M., M. C. Frank, and C. M. Bitz, 2019: Sea ice loss in association with arctic cyclones. *Nat. Geosci.*, **In Preparation**.

Cavallo, S. M. and W. Skamarock, 2017: The wild wild north: Exploring a new frontier in search for extended range prediction. *Arctic Meteorology Meeting*, Seattle, WA, University of Washington.

Cavallo, S. M., W. Skamarock, N. Szapiro, and C. Riedel, 2018: High resolution Arctic models. *Interagency Arctic Research Policy Committee (IARPC)*, Washington, D.C.

Cavallo, S. M. and W. S. Skamarock, 2012: Extended range prediction over the Arctic with the Model for the Prediction Across Scales. *DRI Meeting for Seasonal Prediction*, Monterey, CA, Naval Research Lab.

Cavallo, S. M. and W. S. Skamarock, 2013: Extended range prediction over the Arctic with the Model for the Prediction Across Scales. *DRI Meeting for Seasonal Prediction*, Monterey, CA, Naval Research Lab.

Cavallo, S. M. and W. S. Skamarock, 2014: Extended range prediction over the Arctic with the Model for the Prediction Across Scales. *DRI Meeting for Seasonal Prediction*, Monterey, CA, Naval Research Lab.

Cavallo, S. M. and W. S. Skamarock, 2015: Extended range prediction over the Arctic with the Model for the Prediction Across Scales. *DRI Meeting for Seasonal Prediction*, Monterey, CA, Naval Research Lab.

Cavallo, S. M. and W. S. Skamarock, 2016: Extended range prediction over the Arctic with the Model for the Prediction Across Scales. *DRI Meeting for Seasonal Prediction*, Monterey, CA, Naval Research Lab.

Skamarock, W. S., L. J. Wicker, A. J. Clark, and S. M. Cavallo, 2016: Extended-range severe weather guidance using a global convection-permitting model (invited presentation). *96th American Meteorological Society Annual Meeting*, New Orleans, LA, American Meteorological Society.

Szapiro, N. and S. M. Cavallo, 2013: Simulation of an Arctic summer cyclone using MPAS. *International Symposium on Earth-Science Challenges: The 3rd Summit between the University of Oklahoma and Kyoto University*, Kyoto, Japan.

Szapiro, N. and S. M. Cavallo, 2018: Tpvtrack (v1.0): A watershed segmentation and overlap correspondence method for tracking tropopause polar vortices. *Geoscientific Model Development*, **11 (12)**, 5173–5187.

Szapiro, N., S. M. Cavallo, and W. Skamarock, 2017: Multi-scale Arctic prediction with MPAS-CESM. *CESM Workshop Polar Climate Working Group*, Boulder, CO.

Szapiro, N., S. M. Cavallo, and W. C. Skamarock, 2019a: Can tropopause polar vortices impact Arctic sea ice loss? Part I: Dynamical global model formulation. *Mon. Wea. Rev.*, In Preparation.

Szapiro, N., S. M. Cavallo, and W. C. Skamarock, 2019b: A multi-scale modeling system for regional prediction over the Arctic. *Mon. Wea. Rev.*, In Preparation.

PATENTS

None.

HONORS/AWARDS/PRIZES

- Nicholas Szapiro selected as a Research Scientist at Norwegian Meteorological Institute, Ocean and Ice Division to help design coupled atmosphere-ocean-sea ice model.
- Nicholas Szapiro successfully defended his Ph.D. dissertation entitled "Impacts of tropopause polar vortices on Arctic sea ice loss" at the University of Oklahoma, School of Meteorology 12 March 2019.
- Ph.D. student Nicholas Szapiro awarded the University of Oklahoma Provost's Certificate of Distinction for Outstanding Graduate Teaching Assistant in 2018.
- Ph.D. student Nicholas Szapiro awarded the University of Oklahoma School of Meteorology Oustanding Teaching Assistant Award in 2018.
- Ph.D. student Nicholas Szapiro selected to participate in the 2016 Dynamical Core Model Intercomparison Project at NCAR in Boulder, CO.
- Ph.D. student Nicholas Szapiro invited to give seminar in the Year of Polar Prediction (YOPP) Summit in Geneva, Switzerland 13-15 July 2015.